



1 Riverine impact on future projections of marine primary 2 production and carbon uptake

3 Shuang Gao^{1,2}, Jörg Schwinger³, Jerry Tjiputra³, Ingo Bethke¹, Jens Hartmann⁴, Emilio
4 Mayorga⁵, Christoph Heinze¹

5 ¹Geophysical Institute, University of Bergen, Bjerknes Centre for Climate Research, Norway

6 ²Institute of Marine Research, Bergen, Norway

7 ³NORCE Norwegian Research Centre, Bjerknes Centre for Climate Research, Norway

8 ⁴Institute of Geology, Center for Earth System Research and Sustainability (CEN), Universität Hamburg,
9 Germany

10 ⁵University of Washington, USA

11 *Correspondence to:* Shuang Gao (Shuang.gao@hi.no)

12 **Abstract.** Riverine transport of nutrients and carbon from inland waters to the coastal and finally the open ocean
13 alters marine primary production (PP) and carbon (C) uptake, not only regionally but also globally. So far, this
14 contribution is represented in the state-of-the-art Earth system models with limited effort. Here we assess changes
15 in marine PP and C uptake projected under the Representative Concentration Pathway 4.5 climate scenario using
16 the Norwegian Earth system model, with four riverine configurations: deactivated, fixed at a contemporary level,
17 coupled to simulated freshwater runoff, and following four plausible future scenarios. The inclusion of riverine
18 nutrients and carbon improves the modelled contemporary spatial distribution relative to observations, especially
19 on the continental margins (5.4% reduction in root mean square error [RMSE] for PP) and in the North Atlantic
20 region (7.4% reduction in RMSE for C uptake). Riverine nutrient inputs alleviate nutrient limitation, especially
21 under future warmer conditions as stratification increases, and thus lessen the projected future decline in PP by
22 up to 0.6 PgC yr⁻¹ (27.3%) globally depending on the riverine configuration. The projected C uptake is enhanced
23 along continental margins where increased PP, due to riverine nutrient inputs, dominates over the CO₂ outgassing
24 owing to riverine organic matter inputs. Conversely, where the riverine organic matter inputs dominate over the
25 nutrient inputs, the projected C uptake is reduced. The large range of the riverine input across our four riverine
26 configurations does not transfer to a large uncertainty of the projected global PP and ocean C uptake, suggesting
27 that transient riverine inputs are more important for high-resolution regional studies such as in the North Atlantic
28 and along the continental margins.

29 1 Introduction

30 At global scale, the major sources of both dissolved and particulate materials to the oceans are river runoff,
31 atmospheric deposition and hydrothermal inputs. Of these three, river runoffs play an essential role in transporting
32 nutrients which stimulate biological primary production in the ocean (Meybeck, 1982; Smith et al., 2003; Chester,
33 2012). For some substances such as total phosphorus (TP) and total silicon, riverine input even acts as the
34 absolutely dominant source. River transport of carbon influences the air-sea carbon (C) exchange, local oxygen
35 balance and acidification level, thus further affecting marine ecosystem health. Although riverine carbon only
36 plays a minor role in the global carbon cycle, it is very sensitive to regional and global changes (Meybeck and



37 Vörösmarty, 1999). With an increasing world population and a perturbed hydrological cycle under climate change,
38 riverine transport of nutrients and carbon from land to oceans has a potentially growing impact on the marine
39 biogeochemistry and ecosystem. The impacts of anthropogenic activity, particularly agriculture, wastewater
40 discharges and extensive damming, have greatly perturbed the riverine transport of nitrogen (N), phosphorus (P)
41 and silicon (Si) to the oceans. Seitzinger et al. (2010) estimate that there is an increase in global riverine fluxes of
42 dissolved inorganic nitrogen (DIN) and phosphorus (DIP) by 35% and 29%, respectively, between 1970 and 2000,
43 and a further possible change of -2% to +29% in DIN and +37% to +57% in DIP between 2000 and 2050,
44 depending on the future scenarios used in their study. The riverine carbon input is highly influenced by the
45 magnitude of continental runoff, permafrost melting and leaching of post-glacial peat deposits, all of which are
46 sensitive to climate change. In addition, anthropogenic change, such as land-use and land-cover changes, lake and
47 reservoir eutrophication and sewage emissions of organic material into rivers may become an important factor in
48 the future (Meybeck and Vörösmarty, 1999).

49 However, the contributions of riverine substances and associated processes are not well represented in the state-
50 of-the-art Earth system models (ESMs). Previous modelling studies have either focused on a single riverine
51 species, e.g., C or Si (Aumont et al., 2001; Bernard et al., 2011), or on a confined time period with constant
52 riverine fluxes, e.g. pre-industrial or present-day (Lacroix et al., 2020; Cotrim da Cunha et al., 2007; Bourgeois
53 et al., 2016). Although the riverine transports of nutrients and carbon have been considered in the latest ESMs
54 (e.g., Tjiputra et al., 2020), their impacts on future projections of marine biogeochemistry have not been
55 sufficiently addressed and warrant further investigation. Taking the advantage of the latest improvement of global
56 river nutrient/carbon export datasets and responding to the demand of development of ESMs with increasing
57 model resolution, the assessment of the impact of riverine nutrients and carbon on future projections of marine
58 biogeochemistry becomes feasible and desired, especially for impact studies along continental margins.

59 In this study, we aim to assess the impact of riverine nutrients and carbon on the projected changes in regional
60 and global marine primary production (PP) and air-sea CO₂ exchange by addressing the following questions:

- 61 1) How does the presence of riverine fluxes of nutrient and carbon affect the contemporary representation of
62 marine biogeochemistry in our model?
- 63 2) How does the presence of riverine fluxes of nutrient and carbon affect the future projections of marine
64 biogeochemistry?
- 65 3) How important is the consideration of transient changes in riverine fluxes of nutrient and carbon on the
66 future projections?

67 We explore these questions by performing a series of transient historical and 21st century climate simulations
68 under the RCP 4.5 scenario with the fully coupled Norwegian Earth system model (NorESM) under four different
69 riverine input configurations.



70 **2 Methods**

71 **2.1 Model description**

72 All simulations in this study have been performed with the Norwegian Earth System Model version 1 (NorESM1-
73 ME, hereafter NorESM) (Bentsen et al., 2013), a state-of-the-art climate model that provided input to the Fifth
74 Coupled Model Intercomparison Project (CMIP5) (Taylor et al., 2011). The model is based on the Community
75 Earth System Model version 1 (CESM1) (Hurrell et al., 2013). The atmospheric, land and sea ice components are
76 the Community Atmosphere Model (CAM4) (Neale et al., 2013), the Community Land Model (CLM4) (Oleson
77 et al., 2010; Lawrence et al., 2011) and the Los Alamos National Laboratory sea ice model (CICE4) (Holland et
78 al., 2011), respectively. An interactive aerosol-cloud-chemistry module has been added to the atmospheric
79 component (Kirkevåg et al., 2013). The physical ocean component—the Bergen Layered Ocean Model (BLOM,
80 formerly called NorESM-O) (Bentsen et al., 2013)—is an updated version of the Miami Isopycnic Coordinate
81 Ocean Model (MICOM) (Bleck and Smith, 1990; Bleck et al., 1992) and features a stack of 51 isopycnic layers
82 (potential densities ranging from 1028.2 to 1037.8 kg m⁻³ referenced to 2000 dbar) with a two-layer bulk mixed
83 layer on top. The depth of the bulk mixed layer varies in time and the thickness of the topmost layer is limited to
84 10 m in order to allow for a faster air-sea flux exchange. The ocean and sea ice components are configured on a
85 dipolar curvilinear horizontal grid with a 1° nominal resolution that is enhanced at the Equator and towards the
86 poles, and its northern grid pole singularity is rotated over Greenland. The atmosphere and land components are
87 configured on a regular 1.9° x 2.5° horizontal grid.

88 The ocean biogeochemistry component of NorESM is based on the Hamburg Ocean Carbon Cycle Model
89 (HAMOCC5) (Maier-Reimer et al., 2005). The component has been tightly coupled to NorESM-O such that both
90 components share the same horizontal grid as well as vertical layers and that all tracers are transported by the
91 physical component at model time step (Assmann et al., 2010). Tuning choices and further improvements to the
92 biogeochemistry component are detailed in Tjiputra et al. (2013). Here we only summarise features of particular
93 importance to this study. The partial pressure of CO₂ (*p*CO₂) in seawater is calculated as a function of surface
94 temperature, salinity, pressure, dissolved inorganic carbon (DIC) and total alkalinity. Dissolved iron is released
95 to the surface ocean with a constant fraction (3.5%) of the climatology monthly aerial dust deposition (Mahowald
96 et al., 2005), but only 1% of this is assumed to be bio-available. Nitrogen fixation by cyanobacteria occurs when
97 nitrate in the surface water is depleted relative to phosphate according to the Redfield ratio (Redfield et al., 1934).
98 Phytoplankton growth in the model depends on temperature, availability of light and on the most limiting nutrient
99 among phosphate, nitrate and iron. Constant stoichiometric ratios for the biological fixation of C, N, P and ΔO₂
100 (122 : 16 : 1 : -172) are prescribed in HAMOCC, and are extended by fixed Si : P (25 : 1) and Fe : P (3.66 x 10⁻⁴
101 : 1) stoichiometric ratios. HAMOCC prognostically simulates export production of particulate organic carbon
102 (POC). It is assumed that a fraction of POC production is associated with diatom silica production, and the
103 remaining fraction is associated with calcium carbonate production by coccolithophorides. The fraction of diatom-
104 associated production is calculated from silicate availability, effectively assuming that diatoms are able to out-
105 compete other phytoplankton growth under favorable (high surface silicate concentration) growth conditions.
106 Particles, including POC, biogenic silica, calcium carbonate and dust are advected by ocean circulation in the



107 model. Those particles sink through the water column with constant sinking speeds and are remineralized at
108 constant rates. HAMOCC includes an interactive sediment module with 12 biogeochemically active vertical layers.
109 Permanent burial of particles out of the deepest sediment layer represents a net loss of POC, calcium carbonate
110 and silica from the ocean/sediment system and is compensated by atmospheric and riverine inputs on a time scale
111 of several thousand model-years. The overall performance of the physical and biogeochemistry ocean components
112 has been evaluated elsewhere (Bentsen et al., 2013; Tjiputra et al., 2013). More detailed model description and
113 parameters are documented in the same publications.

114 **2.2 Riverine data implementation**

115 The influx of carbon and nutrients from over 6000 rivers to the coastal oceans has been implemented in HAMOCC
116 based on previous work of Bernard et al. (2011) but with modifications that are outlined in the following
117 paragraphs.

118 The riverine influx includes carbon, nitrogen and phosphorus, each in dissolved inorganic, dissolved organic, and
119 particulate forms, as well as alkalinity (ALK), dissolved silicon and iron (Fe). Except for DIC, ALK and Fe, all
120 data are provided by the Global NEWS 2 (NEWS 2) model (Mayorga et al., 2010), which is a hybrid of empirical,
121 statistical and mechanistic model components that simulate steady-state annual riverine fluxes as a function of
122 natural processes and anthropogenic influences. The NEWS 2 data product contains historical (year 1970 and
123 2000) and future (year 2030 and 2050) estimates of riverine fluxes of carbon and nutrients. The future products
124 are developed based on four Millennium Ecosystem Assessment (MEA) scenarios (Alcamo et al., 2006): Global
125 Orchestration (GNg), Order from Strength (GNo), Technogarden (GNt) and Adapting Mosaic (GNa). These
126 scenarios represent different focuses of future society on e.g. globalization or regionalization, reactive or proactive
127 environmental management and their respective influences on efficiency of nutrient use in agriculture, nutrient
128 release from sewage, total crop and livestock production along with others (Seitzinger et al., 2010).

129 DIC and ALK fluxes are taken from the work of Hartmann (2009). Riverine Fe flux is calculated as a proportion
130 of a global total input of 1.45 Tg yr^{-1} (Chester et al., 1990), weighted by water runoff of each river. Only 1% of
131 the riverine Fe is added to the oceanic dissolved Fe, under the assumption that upto 99% of the fluvial gross
132 dissolved Fe is removed during estuarine mixing (Boyle et al., 1977; Figuères et al., 1978; Sholkovitz and Copland,
133 1981; Shiller and Boyle, 1991).

134 At the river mouths, all fluxes are interpolated to the ocean grid in the same way as the freshwater runoff, which
135 is distributed as a function of river mouth distance with an e-folding length scale of 1000 km and cutoff of 300
136 km.

137 In HAMOCC, organic forms of carbon and nutrients are always coupled through the Redfield ratio. Therefore,
138 the least abundant riverine organic constituent (both dissolved and particulate forms) is determined and added to
139 the modelled dissolved organic carbon (DOC) and DET pools (detritus, particulate organic matter). Any
140 remaining riverine organic matter is then added to its inorganic pool (see also Bernard et al., 2011).



141 2.3 Experimental design

142 The fully coupled NorESM model is spun up for 900 years with external forcings fixed at preindustrial year-1850
143 levels prior to our experiments (Tjiputra et al., 2013). The atmospheric CO₂ mixing ratio is set to 284.7 ppm
144 during the spin-up. Nutrients and oxygen concentrations in the ocean are initialised with the World Ocean Atlas
145 dataset (Garcia et al., 2013a, b). Initial DIC and ALK fields are taken from the Global Data Analysis Project (Key
146 et al., 2004). After 900 years, the ocean physical- and biogeochemical tracer distributions reach quasi-equilibrium
147 states. We extended the spin-up for another 200 years with riverine input for each experiment (except for the
148 reference run) and then performed a set of transient climate simulations for the industrial era and the 21st century
149 (1850-2100). The simulations use external climate forcings that follow the CMIP5 protocol (Taylor et al., 2011).
150 For the historical period (1850-2005), observed time-varying solar radiation, atmospheric greenhouse gas
151 concentrations (including CO₂), natural and anthropogenic aerosols are prescribed. For the future period (2006-
152 2100), the Representative Concentration Pathway (RCP) 4.5 (van Vuuren et al., 2011) is applied. Here, we assume
153 that the middle-of-the-road scenario with some mitigations to be the most representative future scenario. The
154 riverine input configurations employed in this study are summarized in Figure 1. The global total fluxes of each
155 nutrient/carbon species are shown in Figure 2. The experiment configurations are described as follows:

- 156 • REF: Reference run. Riverine nutrient and carbon supply is deactivated.
- 157 • FIX and FIXnoc: Fixed at contemporary level. FIX: A constant riverine nutrient and carbon supply,
158 representative for the year 1970 as provided by NEWS 2, is applied to the model throughout the whole
159 experiment duration. FIXnoc: As FIX but only with nutrients supply, all carbon (DIC, DOC, POC) and
160 alkalinity fluxes are not considered.
- 161 • RUN: Coupled to simulated freshwater runoff. Riverine nutrient and carbon supply representative for the
162 year 1970 is linearly scaled with the on-line simulated freshwater runoff divided by the climatological mean
163 runoff over 1960-1979 of the model. Thus, the inputs follow the seasonality and long-term trend of the
164 simulated runoff. We assume that the nutrient and carbon concentrations in the rivers are constant at the
165 level of 1970, but the fluxes fluctuate with freshwater runoff.
- 166 • GNS: Transient input following future projections of NEWS 2. A constant riverine nutrient and carbon
167 supply representative for year 1970 has been applied from year 1850 to 1970. Between year 1970, 2000,
168 2030 and 2050 the annual riverine supply is linearly interpolated. From year 2050 to 2100 the annual riverine
169 supply is linearly extrapolated. From year 2000, riverine supplies of the four NEWS 2 future scenarios (GNa,
170 GNg, GNo and GNt) are applied.

171 By comparing FIX versus REF we assess how the presence of riverine inputs affect the contemporary marine
172 biogeochemistry representation and also the projected changes. By comparing RUN versus FIX we assess the
173 potential effects of riverine nutrient and carbon long-term trends associated with an intensifying global
174 hydrological cycle on marine biogeochemistry. RUN represents a first step towards coupling riverine nutrient and
175 carbon fluxes to the simulated hydrological cycle. By comparing the GNS configurations versus FIX we assess
176 how plausible, realistic future evolutions in riverine nutrient and carbon fluxes may impact marine
177 biogeochemistry projections. We span the uncertainty in future riverine nutrient and carbon fluxes by considering
178 multiple NEWS 2 scenarios.



179 An important feature of the experimental design is that the marine biogeochemistry does not feedback on the
180 physical climate in our model setup. Consequently, the climate variability and climate trends are the same in all
181 experiments and the interannual variability in the biogeochemical parameters—which is dominantly driven by the
182 physical climate variability—is also virtually the same. Any uncertainty related to internal climate variability is
183 thus effectively removed in the computation of the inter-experiment differences. In this manner, we are able to
184 obtain statistically robust results for short time-slices without having to perform multi-member simulation
185 ensembles for each experiment.

186 3 Results

187 3.1 Effect of including riverine inputs on contemporary marine biogeochemistry

188 We start with assessing how the inclusion of riverine nutrients and carbon affects the contemporary representation
189 of the global marine biogeochemistry in our model by comparing the annual mean output over the years 2003-
190 2012 between the REF and FIX experiments. We also compare with observational estimates to see if the inclusion
191 of riverine nutrients and carbon improves the marine biogeochemistry representation in our model.

192 The annual net primary production (PP) is 40 and 43 PgC yr⁻¹ in the REF and FIX experiments, respectively. The
193 increase of PP in FIX occurs along continental margins (where seafloor is shallower than 300 m), accounting for
194 15% of the global total increase, and predominantly in the North Atlantic (Figure 3c). The simulated global total
195 PP in both REF and FIX are lower than the satellite-based model estimates, including Vertically Generalized
196 Production Model (VGPM), Eppley-VGPM and Carbon-based Production Model (CbPM) over the same time
197 period, ranging from 55 to 61 PgC yr⁻¹ (Behrenfeld and Falkowski, 1997; Westberry et al., 2008). Although the
198 total PP in FIX is still considerably lower than the satellite-based estimates, the inclusion of riverine nutrients and
199 carbon does slightly improve the distribution of PP especially on continental margins (Figure 3), according to our
200 area-weighted root mean square error (RMSE) analysis. The RMSE of REF relative to mean observational
201 estimates (mentioned above) averages 10.7 mol C m⁻² yr⁻¹ globally, while the value of FIX is 10.3 mol C m⁻² yr⁻¹,
202 which is reduced by 3.6%. For the continental margins, the RMSE is reduced by 5.4% from 29.0 mol C m⁻² yr⁻¹
203 in REF to 27.4 mol C m⁻² yr⁻¹ in FIX.

204 The ocean annual net uptake of CO₂ is 2.8 and 2.9 Pg C yr⁻¹ in REF and FIX, respectively, with a FIX-REF
205 difference of 0.09±0.01 Pg C yr⁻¹ equivalent to 3.1±0.1% relative change (note that the 2σ standard errors are
206 small because REF and FIX share the same interannual variability). In FIX the ocean carbon uptake is generally
207 enhanced everywhere except for the upwelling regions of the Southern Ocean and in the subpolar North Atlantic
208 between approximately 50°N-65°N and 60°W-10°W (Figure 4c). To isolate the impact of riverine nutrients input
209 from carbon input, an additional experiment (FIXnoc) was conducted, where the nutrient fluxes are implemented
210 the same as in FIX, while all carbon (DIC, DOC, POC) and alkalinity fluxes are eliminated. As shown in Figure
211 4d, the nutrients input results in more CO₂ uptake not only at large river estuaries but also in the subtropical gyres
212 due to enhanced primary production. In the subpolar North Atlantic and in the Southern Ocean upwelling region,
213 the addition of riverine nutrients leads to enhanced outgassing. This is a remote effect of the generally increased
214 primary production (by 3 PgC yr⁻¹), which leads to more remineralized carbon in deeper water masses. The



215 riverine carbon input, on the other hand, leads to CO₂ outgassing mainly at river estuaries (Figure 4e), but also in
216 a band along the gulf stream extending into the North Atlantic, where it accounts for 18% of the CO₂ outgassing
217 in the subpolar region (50°N-65°N, 60°W-10°W). Along the continental margins the nutrients input increases the
218 CO₂ uptake, while the carbon input has an opposite effect which induces more outgassing. The net effect of both
219 nutrient and carbon inputs shows that the uptake of CO₂ dominates over the outgassing, along the continental
220 margins and in subtropical gyres (Figure 4c). Compared to the observational based estimates of Landschützer et
221 al. (2017) (Figure 4a) and according to our RMSE analysis, the inclusion of riverine nutrients and carbon does
222 not improve the simulated air-sea CO₂ fluxes globally. The RMSE of REF relative to observational estimates
223 averages to 0.834 mol C m⁻² yr⁻¹ globally, while the value of FIX is 0.833 mol C m⁻² yr⁻¹. However, there is a
224 distinguishable improvement of the distribution of air-sea CO₂ fluxes in the subpolar North Atlantic (RMSE is
225 reduced by 7.4%, from 0.74 mol C m⁻² yr⁻¹ in REF to 0.68 mol C m⁻² yr⁻¹ in FIX), with slight degradations in some
226 other regions (Figure 4c).

227 3.2 Effect of including contemporary riverine inputs on future projections of marine biogeochemistry

228 We now address how the inclusion of riverine nutrient and carbon fluxes affects future projections of marine
229 biogeochemistry by comparing the average output between a future period (2050-2099) and a historical period
230 (1950-1999) of FIX versus REF.

231 In both experiments the future projections of global PP averaged over the years 2050-2099 are lower than their
232 corresponding 1950-1999 averages (Figure 5a). However, when riverine input of nutrient and carbon is included,
233 the projected decrease of global PP is mitigated from -2.24 Pg C yr⁻¹ in REF to -1.93 Pg C yr⁻¹ in FIX (by 13.8%).
234 Spatially, the decrease of PP in REF occurs largely in upwelling regions such as the tropical eastern Pacific and
235 tropical Atlantic, as well as along a latitude band around 40°S (Figure 6a). The riverine inputs alleviate the
236 projected PP decrease in those regions (see further discussion in Section 4.2) and reinforce the projected PP
237 increase in high latitudes (Figure 6b, c). For instance, the future projections of PP in the Arctic Ocean show
238 significant increases in both REF and FIX. Climate change alone (REF, without riverine inputs) almost doubles
239 the simulated PP in the Arctic from 0.08 Pg C yr⁻¹ during 1950-1999 to 0.15 Pg C yr⁻¹ in 2050-2099 (Figure 5b),
240 likely as a consequence of sea ice retreat. FIX, which includes riverine inputs, exhibits a slightly larger absolute
241 Arctic PP increase (from 0.102 to 0.180 Pg C yr⁻¹) albeit somewhat smaller relative increase (~76%) in its future
242 projection (Figure 5b).

243 For global net uptake rate of CO₂, both experiments (REF and FIX) project a significant increase under the RCP4.5
244 (Figure 7a). The inclusion of riverine inputs leads to a slightly higher (~3%) projected increase of 1.280 Pg C yr⁻¹
245 in FIX compared with 1.247 Pg C yr⁻¹ in REF. The increase rate of CO₂ uptake in the Arctic closely follows the
246 global trend (Figure 7b). Spatially, there is a widespread simulated increase in ocean uptake of CO₂ under future
247 climate change except in the subtropical gyres (Figure 8a). Riverine nutrients input slightly increases the projected
248 carbon uptake at large river estuaries, while decreases the projected uptake in subpolar North Atlantic (Figure 8d).



249 3.3 Effect of future changes in riverine inputs on marine biogeochemistry projections

250 Finally, we address how future changes in riverine fluxes of nutrients and carbon affect marine biogeochemistry
251 by comparing the projected changes for the time period 2050-2099 relative to 1950-1999 among FIX, RUN and
252 the four GNS experiments.

253 The future projected decrease of PP in the four GNS averages to $-1.58 \text{ Pg C yr}^{-1}$, which is less in magnitude
254 compared to FIX ($-1.93 \text{ Pg C yr}^{-1}$) and RUN ($-1.82 \text{ Pg C yr}^{-1}$) (Figure 5a). Spatial distributions of projected PP
255 changes in GNS and their respective differences relative to FIX are shown in Figure 9. The latter occur
256 predominantly on the continental shelf in Southeast Asia, where the future projected increase in riverine nutrient
257 load is the largest in the world in GNS (Seitzinger et al., 2010). Interestingly, the projected increase in PP in
258 Southeast Asia, induced by riverine nutrient inputs in GNS, is of the same order of magnitude as the projected
259 decrease in PP due to future climate change in REF. Thus, in GNS the PP are projected to slightly increase on the
260 continental shelf of Southeast Asia (Figure 9a-d). The riverine nutrient induced PP increase in FIX or RUN is not
261 large enough to compensate the PP decline due to climate change, since the projected changes in riverine nutrient
262 inputs are not taken into account in FIX or locally underestimated in RUN.

263 On the other hand, the future projected increase in the global uptake of CO_2 in GNS ($1.132 \text{ Pg C yr}^{-1}$ in average)
264 is smaller compared to FIX ($1.280 \text{ Pg C yr}^{-1}$) and RUN ($1.290 \text{ Pg C yr}^{-1}$). Differences emerge along continental
265 margins, especially around large river estuaries (Figure 10e-h), where the dissolved organic matter (DOM), that
266 is projected to increase in GNS, enters the ocean and releases CO_2 to the atmosphere (Seitzinger et al., 2010).

267 Despite the regional differences, there is no significant difference in the projected changes in either globally
268 integrated PP or CO_2 uptake among the four GNS in our model (Figures 5 and 7, see further discussion in Section
269 4.3).

270 4 Discussion

271 4.1 Projected marine biogeochemistry changes

272 The projection of global total PP shows less decrease, if riverine inputs are present in the model. We argue that
273 this is mainly because the riverine nutrient inputs into the surface ocean alleviates the increasing nutrient limitation
274 caused by stronger stratification under future climate warming.

275 In our model, PP is roughly linearly related to the concentrations of the most limiting nutrient (Nut), light intensity
276 (I), temperature (T) and the available phytoplankton concentration (Phy), i.e., $\text{PP} \sim \text{Nut} \cdot I \cdot f(T) \cdot \text{Phy}$. It is shown
277 in Figure 6a that under climate change the projected decrease in PP occurs mainly in low- and mid-latitudes.

278 Nitrate is the limiting nutrient (in REF experiment) in almost everywhere except in the Central Indo-Pacific region,
279 in the South Pacific subtropical gyre, in the Bering Sea and part of the Arctic, where Fe is limiting (Figure A1).

280 Projected reduction in surface nitrate concentrations (Figure A2c), which is tightly linked to the upper-ocean
281 warming and increased vertical stratification (Bopp et al., 2001; Behrenfeld et al. 2006; Steinacher et al., 2010;
282 Cabré et al., 2015), contributes to the projected decrease in PP in our model. The simulated global mean PP over
283 2050-2099 is $38.9 \text{ Pg C yr}^{-1}$ in REF, which is $2.24 \text{ Pg C yr}^{-1}$ lower than the value over 1950-1999. This -5.4%
284 projected change in PP is comparable with the multi-model mean estimate of projected change of $-3.6 (\pm 5.7) \%$



285 in the 2090s relative to the 1990s for RCP4.5 (Bopp et al., 2013) and sits in the range of 2-13% decrease projected
286 by four ESMs over the 21st century under the SRES A2 scenario (Steinacher et al., 2010).
287 When riverine nutrient fluxes are added into coastal surface waters in FIX, the PP is higher in both historical and
288 future periods compared to REF (Figure 5a), due to alleviated nutrient limitation. Interestingly, the effect of
289 riverine inputs on PP for the historical and future time period is not the same, suggesting a different nutrient
290 depletion level. The projected decrease in PP is lessened from -5.4% in REF to -4.4% in FIX. We conjecture that
291 during 1950-1999 the riverine nutrients are not depleted by primary producers, while during 2050-2099 the
292 riverine nutrients are utilized to a greater extent due to the exacerbated nutrient limitation and potentially to higher
293 phytoplankton growth rate in warmer climate. Figure 12 illustrates this in a schematic diagram that shows the
294 impact of riverine nutrients on projected PP in low- and mid-latitudes. Moreover, the inclusion of constant riverine
295 inputs (FIX) can potentially explain one tenth of the ~10% (2-13%, Steinacher et al., 2010) inter-model spread.
296 In contrast to the global PP, there are considerable increases in the future projected PP in the Arctic in REF (Figure
297 5b). In polar regions light and temperature are the primary limiting factors for phytoplankton growth, therefore
298 PP increases when light and temperature become more favourable owing to sea-ice melting under warmer
299 conditions (Sarmiento et al., 2004; Bopp et al., 2005; Doney, 2006; Steinacher et al., 2010). On the other hand,
300 the fresher and warmer surface water increases stratification, which counteracts the increase in PP. Therefore,
301 when riverine nutrients input is present in the model, it helps to sustain the projected PP increase in the Arctic,
302 although this effect is only minor (Figure 5b).
303 The ocean annual net uptake of CO₂ increases significantly during 2050-2099 compared with the uptake during
304 1950-1999 in REF (Figure 7a), which is mainly driven by increasing difference in air-sea partial pressure of CO₂.
305 Our experiments show that riverine nutrient inputs have a dominant role over the organic matter inputs in FIX,
306 enhancing CO₂ uptake along continental margins via sustaining PP in both historical and future time periods.

307 **4.2 Different riverine configurations**

308 By exploring different riverine configurations (FIX, RUN, GNS) we investigate how uncertainties in future
309 riverine fluxes translate into uncertainties in projected biogeochemistry changes. In RUN we assume constant
310 concentrations (at 1970's level) of riverine nutrient and carbon over time and couple them to the simulated
311 freshwater runoff. Thus, the annual global total fluxes of nutrient and carbon vary with time following the
312 variability of runoff (Figure 2), in contrast to the constant fluxes in FIX. The global total simulated runoff, under
313 RCP4.5 in our model, is on average higher during 2050-2099 than the runoff during 1950-1999, indicating an
314 intensified hydrological cycle under future climate change. Hence, the global riverine fluxes of nutrient and carbon
315 during 2050-2099 are higher than those during 1950-1999 in RUN. However, the temporal changes in global
316 riverine fluxes in RUN are relatively small compared with the absolute flux values in FIX, which explains the
317 slightly larger projected changes in global PP and ocean carbon uptake in RUN compared to FIX. It is noteworthy
318 that the large inter-annual variability in the riverine fluxes of nutrient and carbon in RUN does not increase the
319 inter-annual variability in simulated PP and ocean carbon uptake either globally or on the continental margins
320 (Figure 11), something that warrants further investigation. The approach of RUN serves as the first step towards
321 time-varying riverine inputs that take the hydrological variability into account. It can be utilised in future efforts



322 assessing seasonal and inter-annual effects of riverine inputs on regional scale in high-resolution models with
323 better representation of shelf processes. Although the RUN approach is more advanced compared to FIX, it
324 employs a linear relationship between the future riverine nutrient and carbon fluxes and simulated hydrological
325 cycle, which is a highly simplified assumption (see discussion in section 4.3).

326 Figure 2 shows that the inputs of DIN and DIP are considerably lower, while the dissolved silicon (DSi) and
327 particulate organic matter (POM) are higher in the future period in RUN compared to GNS. This is because many
328 anthropogenic processes that are important for determining the future riverine fluxes are not considered in RUN,
329 but are considered in NEWS 2 model system, from which the GNS' future scenarios are simulated. For example,
330 the nutrient management in agriculture, the sewage treatment and phosphorus detergent use, and the increased
331 reservoirs from global dam construction in river system (Seitzinger et al., 2010; Beusen et al., 2009) are the key
332 factors affecting future riverine fluxes of DIN, DIP, and DSi/POM, respectively. Therefore, it is worth exploring
333 the merits of using GNS in future projections of marine biogeochemistry. The four future scenarios provide a
334 range of potential outcomes resulting from different choices tending toward either globalization or regional
335 orientation, either reactive or proactive approach to environmental threats. Surprisingly, even a large range of the
336 riverine inputs in GNS, e.g., temporal changes in DIN fluxes across scenarios ranging 24.8-63.0% of the annual
337 flux in FIX, do not transfer to large uncertainties in future global marine biogeochemistry projections in NorESM.
338 However, the scenario differences might be of importance in regional projections, such as in seas surrounded by
339 highly populated nations and near river estuaries. Simulations with high-resolution global or regional models with
340 a good representation of shelf processes are required to accurately assess the local impact of riverine inputs.

341 **4.3 Limitations and uncertainties**

342 Given that the riverine nutrient and carbon inputs account for only a small proportion of the total amount of
343 nutrients and carbon in the euphotic zone of the ocean, we acknowledge several limitations of our study,
344 particularly related to the complexity and resolution of our ESM. Firstly, shelf processes, which are not well
345 represented in our model, modify a large fraction of some riverine species, e.g., conversion of organic carbon to
346 CO₂ occurs rapidly via remineralization in estuaries before they are transported to the open ocean. Secondly,
347 coarse-resolution models tend to underestimate primary production along the coast. Such well-known model
348 issues may offset the impact induced by riverine inputs. Moreover, we have conducted all simulations only under
349 one IPCC representative concentration pathway scenario (the intermediate RCP 4.5), which may lead to a
350 narrower possible range of the riverine fluxes induced impact on the projected marine biogeochemistry.

351 In RUN we assume constant concentrations of riverine nutrient and carbon over time and the fluxes vary with
352 freshwater runoff. This may be applicable for some nutrients such as DIN or within a certain limit of runoff change
353 such as for dissolved Si (Figure A3). However, this may not be appropriate for all nutrient/carbon species.
354 Furthermore, the variability of runoff is subject to interannual to decadal climate variability, which partially masks
355 the centennial trend. This caveat can be overcome through performing multi-realization ensemble simulations.



356 5 Conclusions

357 In this study, we apply a fully coupled Earth system model to assess the impact of riverine nutrients and carbon
358 delivery to the ocean on the contemporary and future marine primary production and carbon uptake. We also
359 quantify the effects of uncertainty in future riverine fluxes on the projected changes, using several riverine input
360 configurations.

361 Compared to satellite- and observation-based estimates, the inclusion of riverine nutrients and carbon improves
362 the contemporary spatial distribution only slightly on a global scale (3.6% and 0.1% reduction in RMSE for PP
363 and ocean carbon uptake, respectively), with larger improvements on the continental margins (5.4% reduction in
364 RMSE for PP) and the North Atlantic region (7.4% reduction in RMSE for carbon uptake).

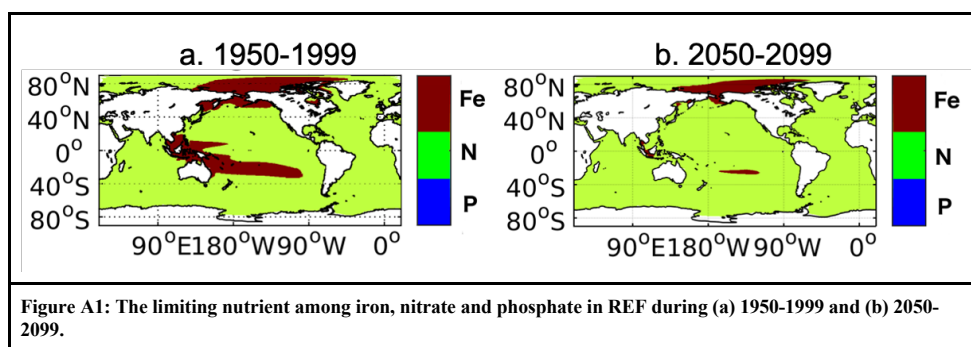
365 Concerning future projected changes, decline in nutrients supply in tropical and subtropical surface waters, due
366 to upper ocean warming and increased vertical stratification, is projected by our model to reduce PP over the 21st
367 century. Riverine nutrient inputs into surface coastal waters alleviate the nutrient limitation and considerably
368 lessen the projected future decline in PP from -5.4% without riverine inputs to -4.4%, -4.1% and -3.6% in FIX,
369 RUN and GNS (averaged over four scenarios), respectively. Different from the global value, the projected PP in
370 the Arctic increases considerably, because light and temperature—the primary limiting factors for phytoplankton
371 growth in polar regions—become more favourable due to sea-ice melting under warmer future conditions. When
372 riverine nutrient inputs are presented in the model, they further enhance the projected increase in PP in the Arctic,
373 counteracting the nutrient decline effect due to stronger stratification in the fresher and warmer surface water.

374 Depending on the riverine scenarios, where the riverine nutrient inputs dominate over the organic matter, the
375 projected net uptake of CO₂ further enhances along continental margins via photosynthesis process. Conversely,
376 where the riverine organic matter inputs are dominant over the nutrient inputs, the projected net uptake of CO₂ is
377 reduced, especially at large river estuaries, due to higher CO₂ outgassing.

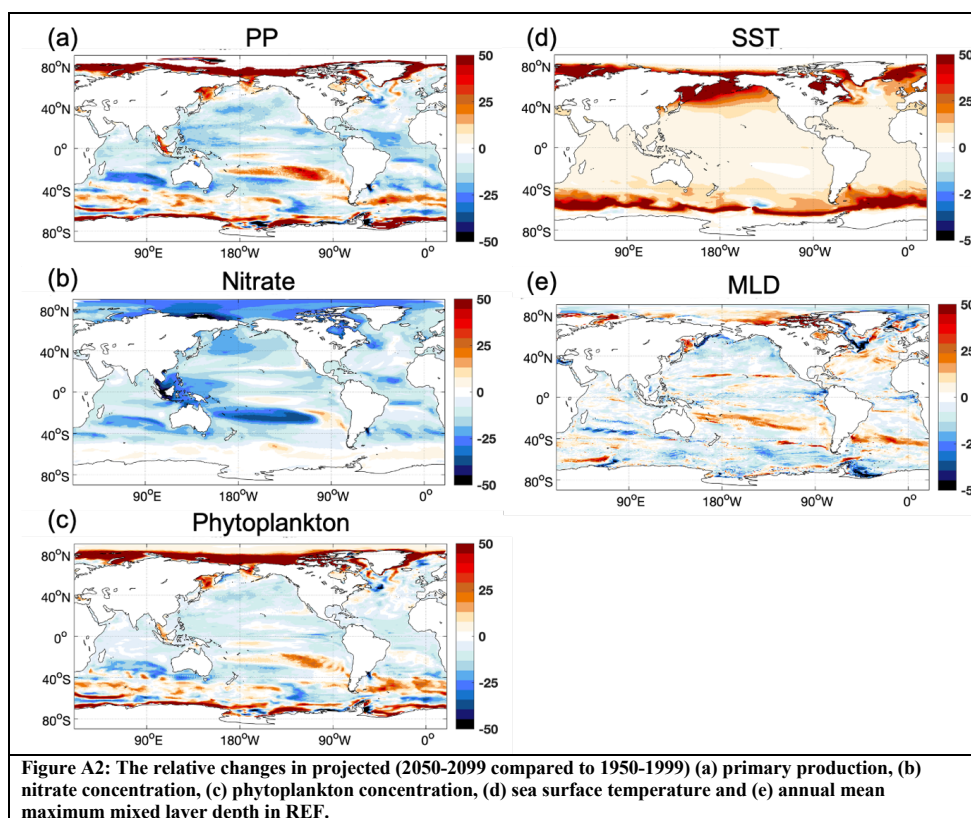
378 We have explored a range of riverine input configurations from temporally constant fluxes (FIX), to idealised
379 time-varying fluxes following variations in simulated hydrological cycle (RUN), to plausible future scenarios
380 (GNS) from a set of global assumptions. The large range of the uncertainty of the riverine input does not transfer
381 to large uncertainty of the projected global PP and ocean carbon uptake. Our study suggests that applying transient
382 riverine inputs in the ESMs with coarse or intermediate model resolution (~1°) does not significantly reduce the
383 uncertainty in global marine biogeochemistry projections, but it may be of importance for regional studies such
384 as in the North Atlantic and along the continental margins.



385 Appendix A



386
387



388

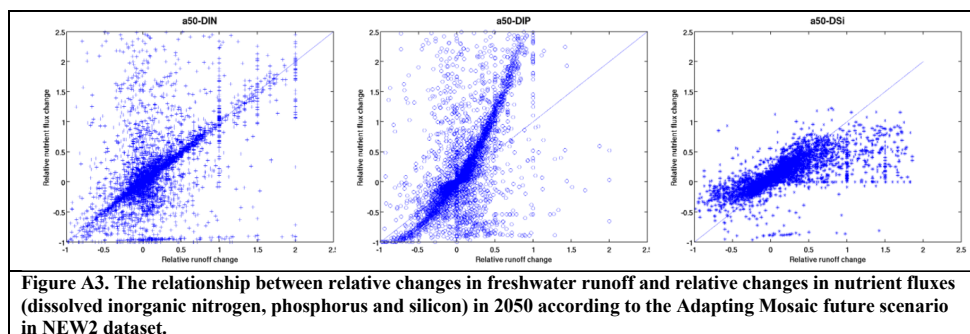


Figure A3. The relationship between relative changes in freshwater runoff and relative changes in nutrient fluxes (dissolved inorganic nitrogen, phosphorus and silicon) in 2050 according to the Adapting Mosaic future scenario in NEW2 dataset.

389 **Code and data availability**

390 The model code and riverine data used can be provided by the corresponding author upon request.

391 **Author contribution**

392 SG and IB designed the model experiments and SG developed the model code and performed the simulations with
393 the help from IB. JS and JT contributed to the interpretation and analysis of the results. JS, JT, IB and CH
394 contributed to editing the manuscript. CH supervised the project work. JH and EM provided riverine data and
395 consultation. SG prepared the manuscript with contributions from all co-authors.

396 **Competing interests**

397 The authors declare that they have no conflict of interest.

398 **Disclaimer**

399 This article reflects only the authors' view – the funding agencies as well as their executive agencies are not
400 responsible for any use that may be made of the information that the article contains.

401 **Acknowledgement**

402 This work was supported through project CRESCENDO (Coordinated Research in Earth Systems and
403 Climate: Experiments, kNowledge, Dissemination and Outreach; Horizon 2020 European Union's Framework
404 Programme for Research and Innovation, grant no. 641816, European Commission). Computing and storage
405 resources have been provided by UNINETT Sigma2 (nn2345k, nn2980k ns2345k, ns2980k). JT acknowledge the
406 Research Council Funded project Downscaling Climate and Ocean Change to Services (CE2COAST; 318477).
407 IB received funding from the Trond Mohn Foundation through the Bjerknes Climate Prediction Unit
408 (BFS2018TMT01) and NFR Climate Futures (309562). JH benefited from financial support from the Deutsche



409 Forschungsgemeinschaft (DFG, German Research Foundation) under Germany's Excellence Strategy – EXC
410 2037 'Climate, Climatic Change, and Society' – project number 390683824, contribution to the Center for Earth
411 System Research and Sustainability (CEN) of Universität Hamburg.

412 References

- 413 Alcamo, J., van Vuuren, D., Rosegrant, M., Alder, J., Bennett, E., Lodge, D., Masui, T., Morita, T., Ringler,
414 C., Sala, O., Schulze, K., Zurek, M., Eickhout, B., Maerker, M., and Kok, K.: Changes in ecosystem
415 services and their drivers across the scenarios, in: *Ecosystems and Human Well-being: Scenarios*, edited by:
416 Carpenter, S. R., Pingali, P. L., Bennett, E. M., and Zurek, M. B., Island Press, Washington, 279-354, 2006.
- 417 Assmann, K. M., Bentsen, M., Segschneider, J., and Heinze, C.: An isopycnic ocean carbon cycle model,
418 *Geosci. Model Dev.*, 3, 143-167, 10.5194/gmd-3-143-2010, 2010.
- 419 Aumont, O., Orr, J. C., Monfray, P., Ludwig, W., Amiotte-Suchet, P., and Probst, J.-L.: Riverine-driven
420 interhemispheric transport of carbon, *Global Biogeochemical Cycles*, 15, 393-405,
421 <https://doi.org/10.1029/1999GB001238>, 2001.
- 422 Behrenfeld, M. J. and Falkowski, P. G.: Photosynthetic rates derived from satellite-based chlorophyll
423 concentration, *Limnology and Oceanography*, 42, 1-20, <https://doi.org/10.4319/lo.1997.42.1.0001>, 1997.
- 424 Behrenfeld, M. J., O'Malley, R. T., Siegel, D. A., McClain, C. R., Sarmiento, J. L., Feldman, G. C.,
425 Milligan, A. J., Falkowski, P. G., Letelier, R. M., and Boss, E. S.: Climate-driven trends in contemporary
426 ocean productivity, *Nature*, 444, 752-755, 10.1038/nature05317, 2006.
- 427 Bentsen, M., Bethke, I., Debernard, J. B., Iversen, T., Kirkevåg, A., Seland, Ø., Drange, H., Roelandt, C.,
428 Seierstad, I. A., Hoose, C., and Kristjánsson, J. E.: The Norwegian Earth System Model, NorESM1-M –
429 Part 1: Description and basic evaluation of the physical climate, *Geosci. Model Dev.*, 6, 687-720,
430 10.5194/gmd-6-687-2013, 2013.
- 431 Bernard, C. Y., Dürr, H. H., Heinze, C., Segschneider, J., and Maier-Reimer, E.: Contribution of riverine
432 nutrients to the silicon biogeochemistry of the global ocean – a model study, *Biogeosciences*, 8, 551-564,
433 10.5194/bg-8-551-2011, 2011.
- 434 Beusen, A. H. W., Bouwman, A. F., Dürr, H. H., Dekkers, A. L. M., and Hartmann, J.: Global patterns of
435 dissolved silica export to the coastal zone: Results from a spatially explicit global model, *Global
436 Biogeochemical Cycles*, 23, <https://doi.org/10.1029/2008GB003281>, 2009.
- 437 Bleck, R. and Smith, L. T.: A wind-driven isopycnic coordinate model of the north and equatorial Atlantic
438 Ocean: 1. Model development and supporting experiments, *Journal of Geophysical Research: Oceans*, 95,
439 3273-3285, 10.1029/JC095iC03p03273, 1990.
- 440 Bleck, R., Rooth, C., Hu, D., and Smith, L. T.: Salinity-driven Thermocline Transients in a Wind- and
441 Thermohaline-forced Isopycnic Coordinate Model of the North Atlantic, *Journal of Physical Oceanography*,
442 22, 1486-1505, 10.1175/1520-0485(1992)022<1486:SDTTIA>2.0.CO;2, 1992.
- 443 Bopp, L., Monfray, P., Aumont, O., Dufresne, J.-L., Le Treut, H., Madec, G., Terray, L., and Orr, J. C.:
444 Potential impact of climate change on marine export production, *Global Biogeochemical Cycles*, 15, 81-99,
445 <https://doi.org/10.1029/1999GB001256>, 2001.
- 446 Bopp, L., Aumont, O., Cadule, P., Alvain, S., and Gehlen, M.: Response of diatoms distribution to global
447 warming and potential implications: A global model study, *Geophysical Research Letters*, 32,
448 <https://doi.org/10.1029/2005GL023653>, 2005.
- 449 Bopp, L., Resplandy, L., Orr, J. C., Doney, S. C., Dunne, J. P., Gehlen, M., Halloran, P., Heinze, C., Ilyina,
450 T., Séférian, R., Tjiputra, J., and Vichi, M.: Multiple stressors of ocean ecosystems in the 21st century:
451 projections with CMIP5 models, *Biogeosciences*, 10, 6225-6245, 10.5194/bg-10-6225-2013, 2013.
- 452 Bourgeois, T., Orr, J. C., Resplandy, L., Terhaar, J., Ethé, C., Gehlen, M., and Bopp, L.: Coastal-ocean
453 uptake of anthropogenic carbon, *Biogeosciences*, 13, 4167-4185, 10.5194/bg-13-4167-2016, 2016.



- 454 Boyle, E. A., Edmond, J. M., and Sholkovitz, E. R.: The mechanism of iron removal in estuaries, *Geochim*
455 *Cosmochim Ac*, 41, 1313-1324, [https://doi.org/10.1016/0016-7037\(77\)90075-8](https://doi.org/10.1016/0016-7037(77)90075-8), 1977.
- 456 Cabré, A., Marinov, I., and Leung, S.: Consistent global responses of marine ecosystems to future climate
457 change across the IPCC AR5 earth system models, *Climate Dynamics*, 45, 1253-1280, [10.1007/s00382-](https://doi.org/10.1007/s00382-014-2374-3)
458 014-2374-3, 2015.
- 459 Chester, R.: The transport of material to the oceans: the river pathway, in: *Marine Geochemistry*, Springer,
460 Dordrecht, https://doi.org/10.1007/978-94-010-9488-7_3, 1990.
- 461 Chester, R.: The Input of Material to the Ocean Reservoir, in: *Marine Geochemistry*, Wiley Online Books,
462 7-10, <https://doi.org/10.1002/9781118349083.ch2>, 2012.
- 463 Cotrim da Cunha, L., Buitenhuis Erik, T., Le Quéré, C., Giraud, X., and Ludwig, W.: Potential impact of
464 changes in river nutrient supply on global ocean biogeochemistry, *Global Biogeochemical Cycles*, 21,
465 10.1029/2006GB002718, 2007.
- 466 Doney, S. C.: Plankton in a warmer world, *Nature*, 444, 695-696, [10.1038/444695a](https://doi.org/10.1038/444695a), 2006.
- 467 Figuères, G., Martin, J. M., and Meybeck, M.: Iron behaviour in the Zaire estuary, *Netherlands Journal of*
468 *Sea Research*, 12, 329-337, [https://doi.org/10.1016/0077-7579\(78\)90035-2](https://doi.org/10.1016/0077-7579(78)90035-2), 1978.
- 469 Garcia, H. E., Locarnini, R. A., Boyer, T. P., Antonov, J. I., Baranova, O. K., Zweng, M. M., Reagan, J. R.,
470 and Johnson, D. R.: World Ocean Atlas 2013. Vol. 4: Dissolved Inorganic Nutrients
471 (phosphate, nitrate, silicate), NOAA Atlas NESDIS 76, 25 pp, 2013a.
- 472 Garcia, H. E., Locarnini, R. A., Boyer, T. P., Antonov, J. I., Mishonov, A. V., Baranova, O. K., Zweng, M.
473 M., Reagan, J. R., and Johnson, D. R.: World Ocean Atlas 2013. Vol. 3: Dissolved Oxygen, Apparent
474 Oxygen Utilization, and Oxygen Saturation, NOAA Atlas NESDIS 75, 27 pp, 2013b.
- 475 Hartmann, J.: Bicarbonate-fluxes and CO₂-consumption by chemical weathering on the Japanese
476 Archipelago — Application of a multi-lithological model framework, *Chemical Geology*, 265, 237-271,
477 <https://doi.org/10.1016/j.chemgeo.2009.03.024>, 2009.
- 478 Holland, M. M., Bailey, D. A., Briegleb, B. P., Light, B., and Hunke, E.: Improved Sea Ice Shortwave
479 Radiation Physics in CCSM4: The Impact of Melt Ponds and Aerosols on Arctic Sea Ice, *Journal of*
480 *Climate*, 25, 1413-1430, [10.1175/JCLI-D-11-00078.1](https://doi.org/10.1175/JCLI-D-11-00078.1), 2011.
- 481 Hurrell, J. W., Holland, M. M., Gent, P. R., Ghan, S., Kay, J. E., Kushner, P. J., Lamarque, J. F., Large, W.
482 G., Lawrence, D., Lindsay, K., Lipscomb, W. H., Long, M. C., Mahowald, N., Marsh, D. R., Neale, R. B.,
483 Rasch, P., Vavrus, S., Vertenstein, M., Bader, D., Collins, W. D., Hack, J. J., Kiehl, J., and Marshall, S.:
484 The Community Earth System Model: A Framework for Collaborative Research, *Bulletin of the American*
485 *Meteorological Society*, 94, 1339-1360, [10.1175/BAMS-D-12-00121.1](https://doi.org/10.1175/BAMS-D-12-00121.1), 2013.
- 486 Key, R. M., Kozyr, A., Sabine, C. L., Lee, K., Wanninkhof, R., Bullister, J. L., Feely, R. A., Millero, F. J.,
487 Mordy, C., and Peng, T. H.: A global ocean carbon climatology: Results from Global Data Analysis Project
488 (GLODAP), *Global Biogeochemical Cycles*, 18, <https://doi.org/10.1029/2004GB002247>, 2004.
- 489 Kirkevåg, A., Iversen, T., Seland, Ø., Hoose, C., Kristjánsson, J. E., Struthers, H., Ekman, A. M. L., Ghan,
490 S., Griesfeller, J., Nilsson, E. D., and Schulz, M.: Aerosol–climate interactions in the Norwegian Earth
491 System Model – NorESM1-M, *Geosci. Model Dev.*, 6, 207-244, [10.5194/gmd-6-207-2013](https://doi.org/10.5194/gmd-6-207-2013), 2013.
- 492 Lacroix, F., Ilyina, T., and Hartmann, J.: Oceanic CO₂ outgassing and biological production hotspots
493 induced by pre-industrial river loads of nutrients and carbon in a global modeling approach,
494 *Biogeosciences*, 17, 55-88, [10.5194/bg-17-55-2020](https://doi.org/10.5194/bg-17-55-2020), 2020.
- 495 Landschützer, P., Gruber, N., and Bakker, D.: An updated observation-based global monthly gridded sea
496 surface pCO₂ and air-sea CO₂ flux product from 1982 through 2015 and its monthly climatology.
497 (website: https://www.nodc.noaa.gov/ocads/oceans/SPCO2_1982_2015_ETH_SOM_FFNN.html), 2017.
- 498 Lawrence, D. M., Oleson, K. W., Flanner, M. G., Thornton, P. E., Swenson, S. C., Lawrence, P. J., Zeng,
499 X., Yang, Z.-L., Levis, S., Sakaguchi, K., Bonan, G. B., and Slater, A. G.: Parameterization improvements
500 and functional and structural advances in Version 4 of the Community Land Model, *Journal of Advances in*
501 *Modeling Earth Systems*, 3, [10.1029/2011MS00045](https://doi.org/10.1029/2011MS00045), 2011.



- 502 Mahowald, N. M., Baker, A. R., Bergametti, G., Brooks, N., Duce, R. A., Jickells, T. D., Kubilay, N.,
503 Prospero, J. M., and Tegen, I.: Atmospheric global dust cycle and iron inputs to the ocean, *Global*
504 *Biogeochemical Cycles*, 19, 10.1029/2004GB002402, 2005.
- 505 Maier-Reimer, E., Kriest, I., Segsneider, J., and Wetzell, P.: The Hamburg oceanic carbon cycle
506 circulation model HAMOCC5.1—Technical Description Release 1.1, Tech. Rep. 14, Reports on Earth
507 System Science, Max Planck Institute for Meteorology, Hamburg, Germany, 2005.
- 508 Mayorga, E., Seitzinger, S. P., Harrison, J. A., Dumont, E., Beusen, A. H. W., Bouwman, A. F., Fekete, B.
509 M., Kroeze, C., and Van Drecht, G.: Global Nutrient Export from WaterSheds 2 (NEWS 2): Model
510 development and implementation, *Environmental Modelling & Software*, 25, 837-853,
511 <https://doi.org/10.1016/j.envsoft.2010.01.007>, 2010.
- 512 Meybeck, M.: Carbon, nitrogen, and phosphorus transport by world rivers, *American Journal of Science*,
513 282, 401, 10.2475/ajs.282.4.401, 1982.
- 514 Meybeck, M. and Vörösmarty, C.: Global transfer of carbon by rivers, *Global Change Newsletter*, 37, 18-
515 19, 1999.
- 516 Neale, R. B., Richter, J., Park, S., Lauritzen, P. H., Vavrus, S. J., Rasch, P. J., and Zhang, M.: The Mean
517 Climate of the Community Atmosphere Model (CAM4) in Forced SST and Fully Coupled Experiments,
518 *Journal of Climate*, 26, 5150-5168, 10.1175/JCLI-D-12-00236.1, 2013.
- 519 Oleson, K. W., Lawrence, D. M., Bonan, G. B., Flanner, M. G., Kluzek, E., Lawrence, P. J., Levis, S.,
520 Swenson, S. C., Thornton, P. E., Dai, A., Decker, M., Dickinson, R., Feddema, J., Heald, C. L., Hoffman,
521 F., Lamarque, J.-F., Mahowald, N., Niu, G.-Y., Qian, T., Randerson, J., Running, S., Sakaguchi, K., Slater,
522 A., Stockli, R., Wang, A., Yang, Z.-L., Zeng, X., and Zeng, X.: Technical Description of version 4.0 of the
523 Community Land Model (CLM) (No. NCAR/TN-478+STR), University Corporation for Atmospheric
524 Research, doi:10.5065/D6FB50WZ, 2010.
- 525 Redfield, A. and Daniel, R. J.: On the proportions of organic derivations in sea water and their relation to
526 the composition of plankton, in: James Johnstone Memorial Volume, University Press of Liverpool, 177-
527 192, 1934.
- 528 Sarmiento, J. L., Gruber, N., Brzezinski, M. A., and Dunne, J. P.: High-latitude controls of thermocline
529 nutrients and low latitude biological productivity, *Nature*, 427, 56-60, 2004.
- 530 Seitzinger, S. P., Mayorga, E., Bouwman, A. F., Kroeze, C., Beusen, A. H. W., Billen, G., Van Drecht, G.,
531 Dumont, E., Fekete, B. M., Garnier, J., and Harrison, J. A.: Global river nutrient export: A scenario analysis
532 of past and future trends, *Global Biogeochemical Cycles*, 24, <https://doi.org/10.1029/2009GB003587>, 2010.
- 533 Shiller, A. M. and Boyle, E. A.: Trace elements in the Mississippi River Delta outflow region: Behavior at
534 high discharge, *Geochim Cosmochim Acta*, 55, 3241-3251, [https://doi.org/10.1016/0016-7037\(91\)90486-O](https://doi.org/10.1016/0016-7037(91)90486-O),
535 1991.
- 536 Sholkovitz, E. R. and Copland, D.: The coagulation, solubility and adsorption properties of Fe, Mn, Cu, Ni,
537 Cd, Co and humic acids in a river water, *Geochim Cosmochim Acta*, 45, 181-189,
538 [https://doi.org/10.1016/0016-7037\(81\)90161-7](https://doi.org/10.1016/0016-7037(81)90161-7), 1981.
- 539 Smith, S. V., Swaney, D. P., Talaue-Mcmanus, L., Bartley, J. D., Sandhei, P. T., McLaughlin, C. J., Dupra,
540 V. C., Crossland, C. J., Buddemeier, R. W., Maxwell, B. A., and Wulff, F.: Humans, Hydrology, and the
541 Distribution of Inorganic Nutrient Loading to the Ocean, *BioScience*, 53, 235-245, 10.1641/0006-
542 3568(2003)053[0235:HHATDO]2.0.CO;2, 2003.
- 543 Steinacher, M., Joos, F., Frolicher, T. L., Bopp, L., Cadule, P., Cocco, V., Doney, S. C., Gehlen, M.,
544 Lindsay, K., Moore, J. K., Schneider, B., and Segsneider, J.: Projected 21st century decrease in marine
545 productivity: a multi-model analysis, *Biogeosciences*, 7, 979-1005, 2010.
- 546 Taylor, K. E., Stouffer, R. J., and Meehl, G. A.: An Overview of CMIP5 and the Experiment Design,
547 *Bulletin of the American Meteorological Society*, 93, 485-498, 10.1175/BAMS-D-11-00094.1, 2011.
- 548 Tjiputra, J. F., Roelandt, C., Bentsen, M., Lawrence, D. M., Lorentzen, T., Schwinger, J., Seland, Ø., and
549 Heinze, C.: Evaluation of the carbon cycle components in the Norwegian Earth System Model (NorESM),
550 *Geosci. Model Dev.*, 6, 301-325, 10.5194/gmd-6-301-2013, 2013.



551 Tjiputra, J. F., Schwinger, J., Bentsen, M., Morée, A. L., Gao, S., Bethke, I., Heinze, C., Goris, N., Gupta,
552 A., He, Y. C., Olivie, D., Seland, Ø., and Schulz, M.: Ocean biogeochemistry in the Norwegian Earth
553 System Model version 2 (NorESM2), *Geosci. Model Dev.*, 13, 2393-2431, 10.5194/gmd-13-2393-2020,
554 2020.

555 van Vuuren, D. P., Edmonds, J., Kainuma, M., Riahi, K., Thomson, A., Hibbard, K., Hurtt, G. C., Kram, T.,
556 Krey, V., Lamarque, J.-F., Masui, T., Meinshausen, M., Nakicenovic, N., Smith, S. J., and Rose, S. K.: The
557 representative concentration pathways: an overview, *Climatic Change*, 109, 5, 10.1007/s10584-011-0148-z,
558 2011.

559 Westberry, T., Behrenfeld, M. J., Siegel, D. A., and Boss, E.: Carbon-based primary productivity modeling
560 with vertically resolved photoacclimation, *Global Biogeochemical Cycles*, 22,
561 <https://doi.org/10.1029/2007GB003078>, 2008.

562
563

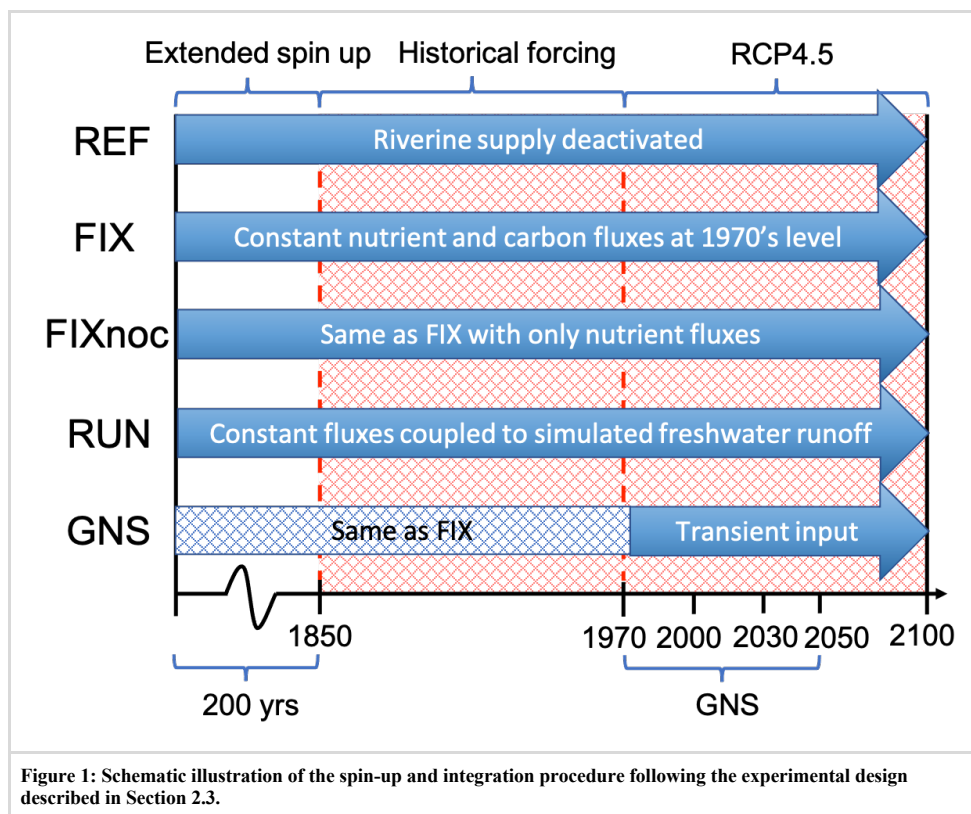
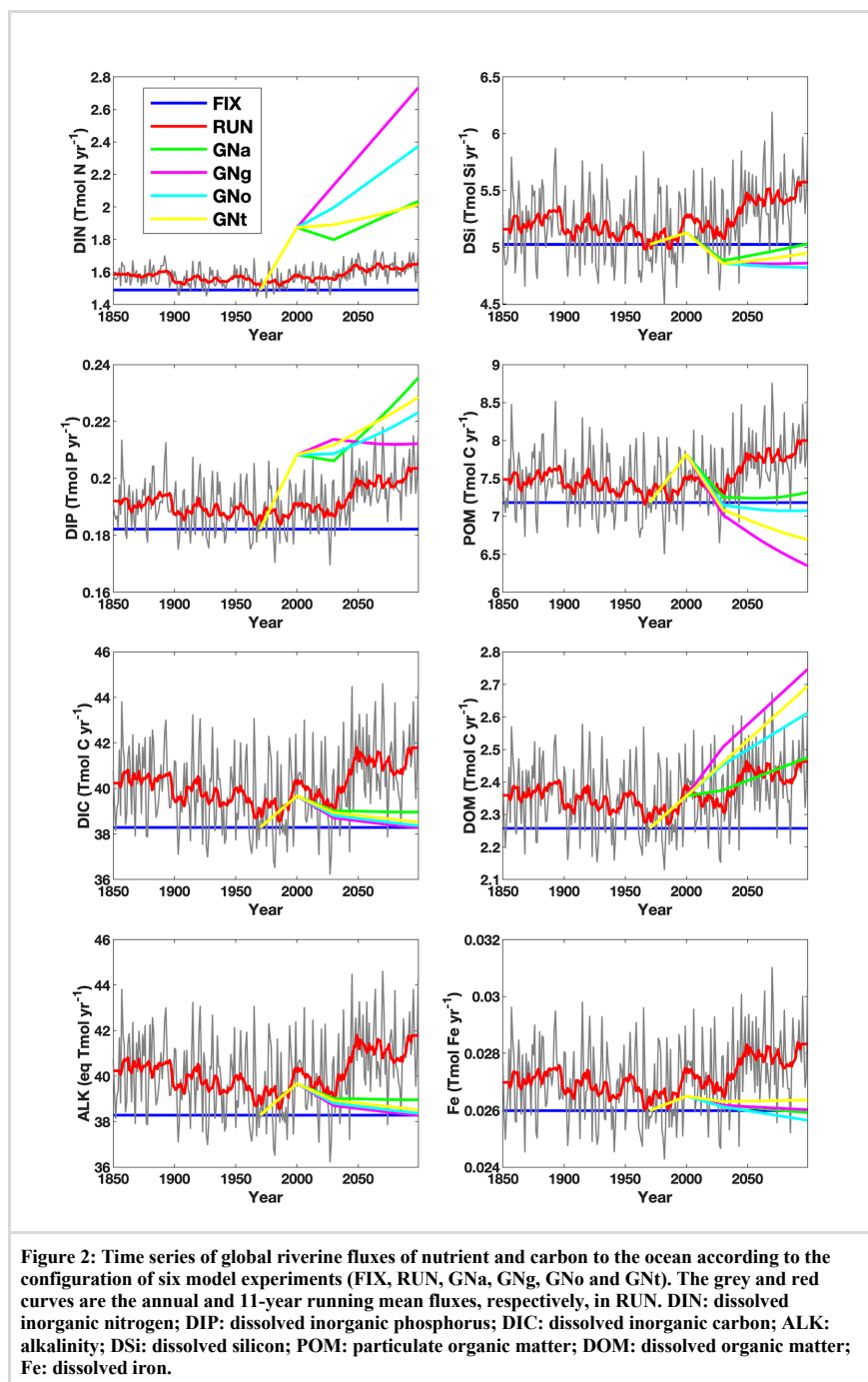


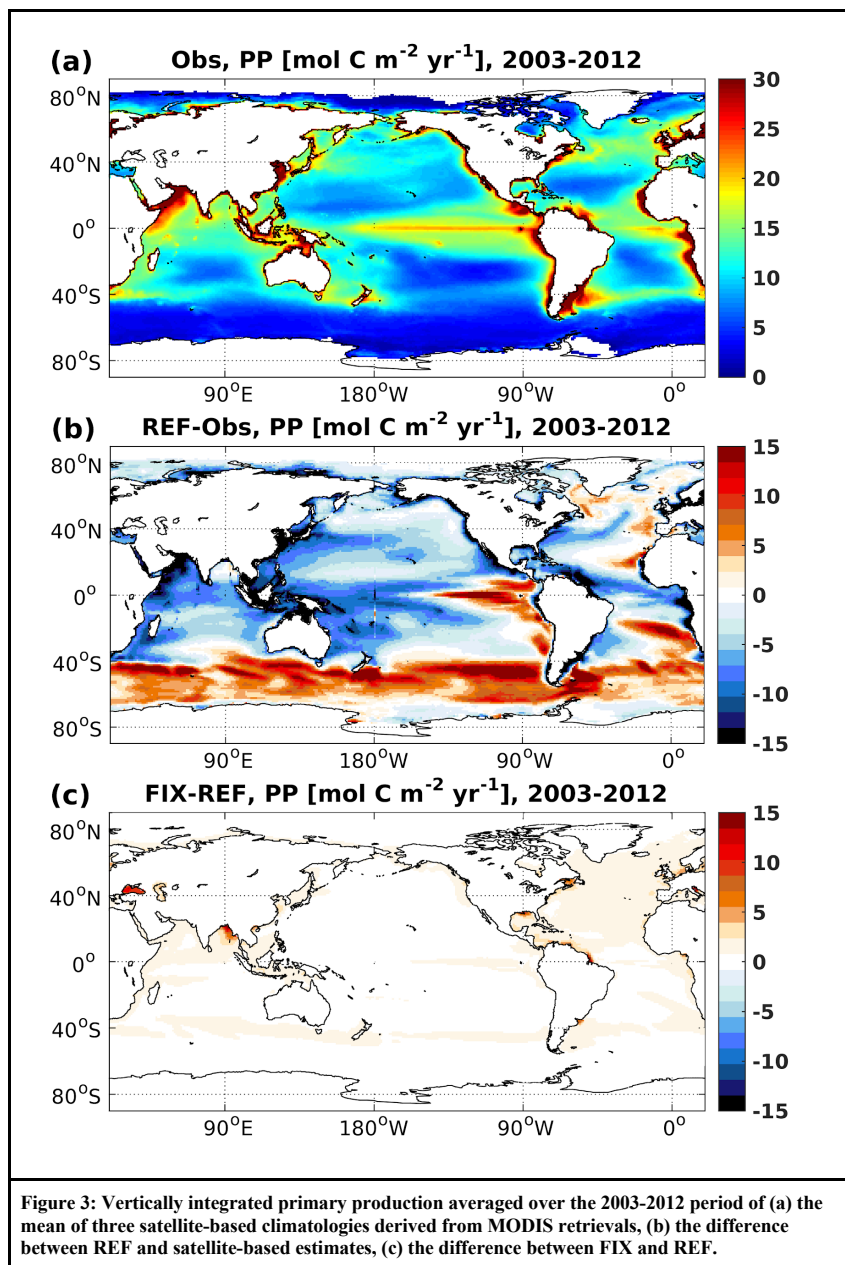
Figure 1: Schematic illustration of the spin-up and integration procedure following the experimental design described in Section 2.3.

564
565

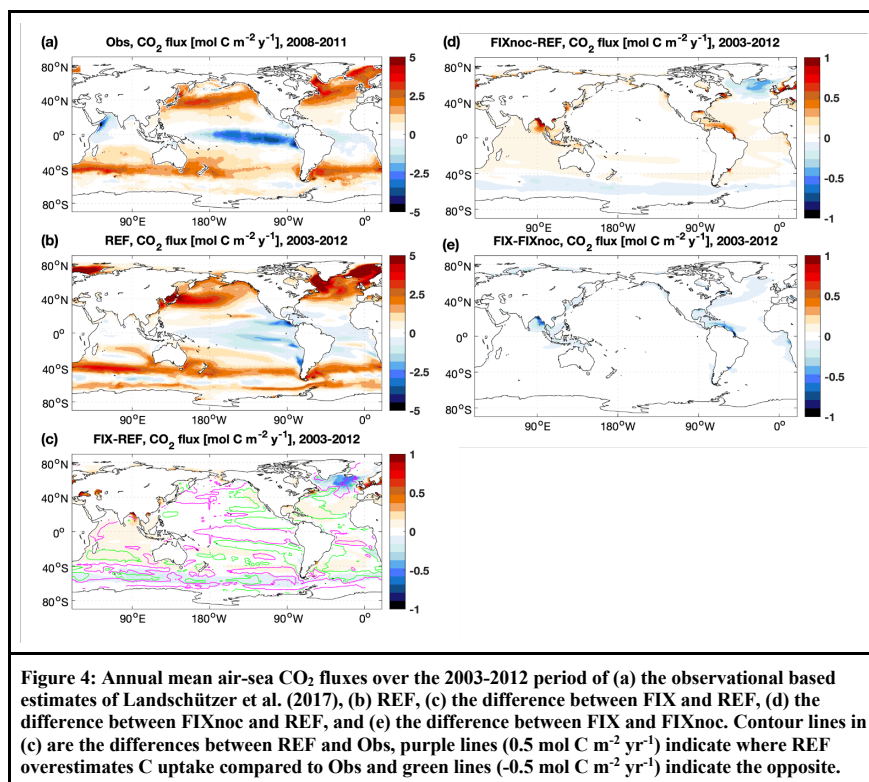




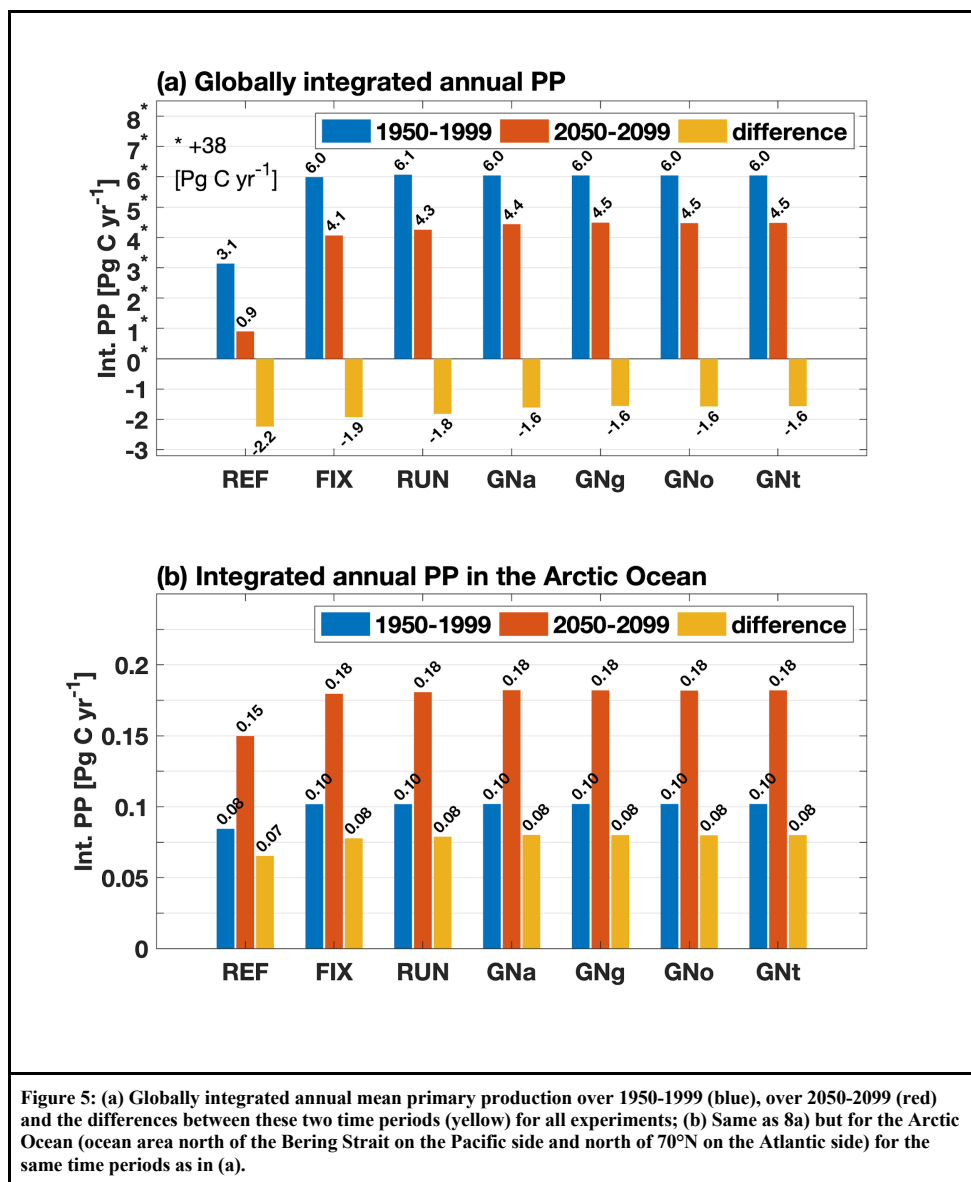
567



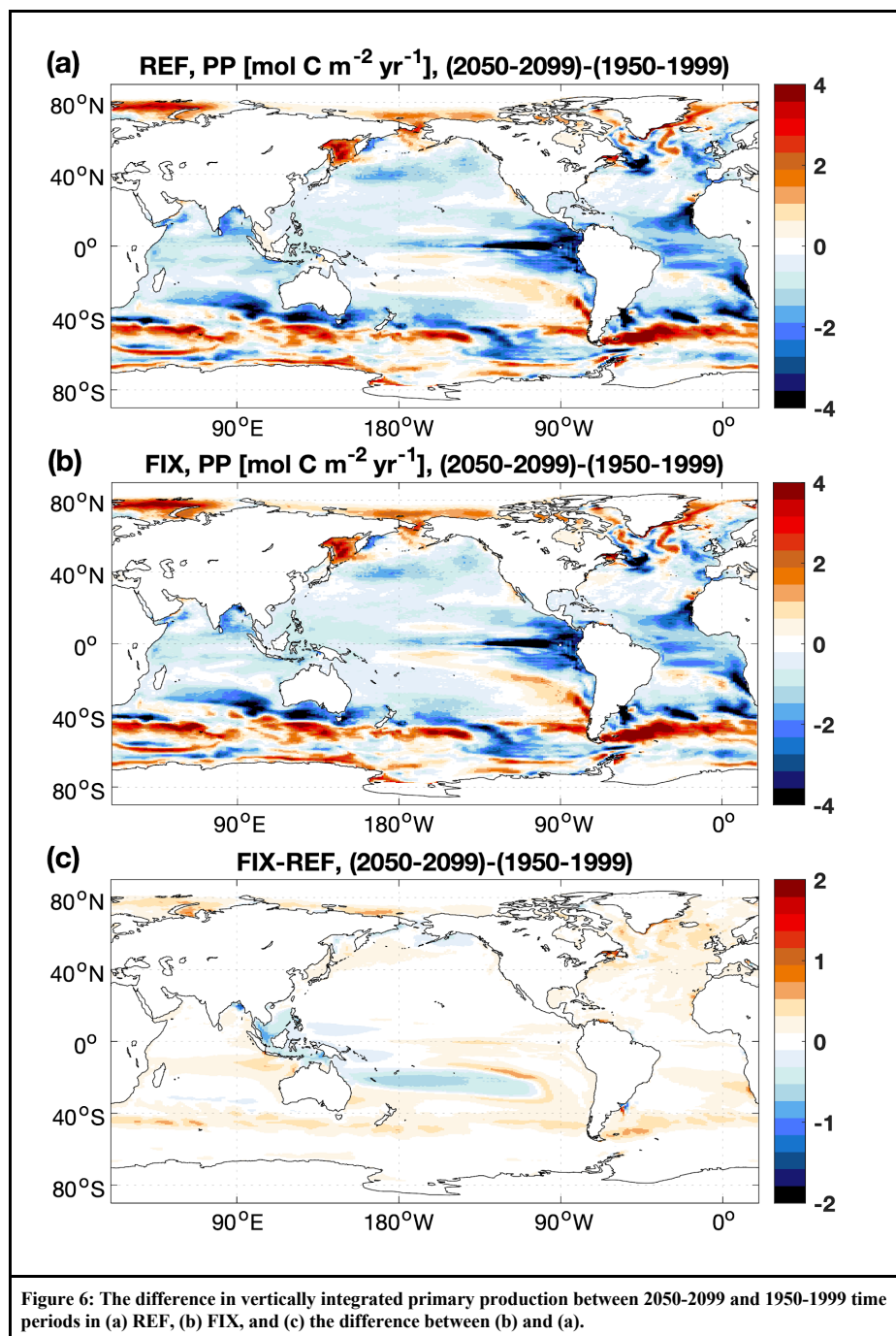
568

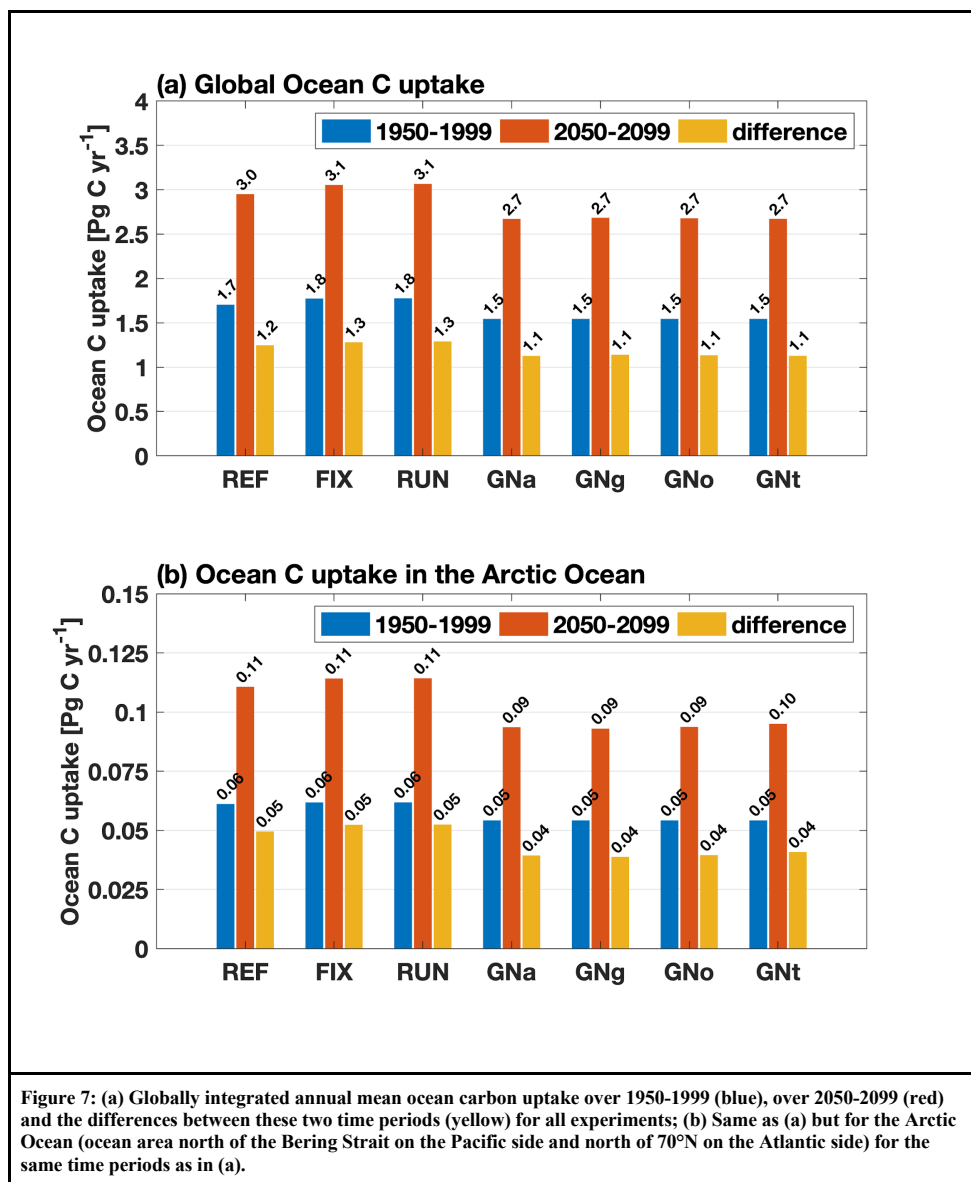


569

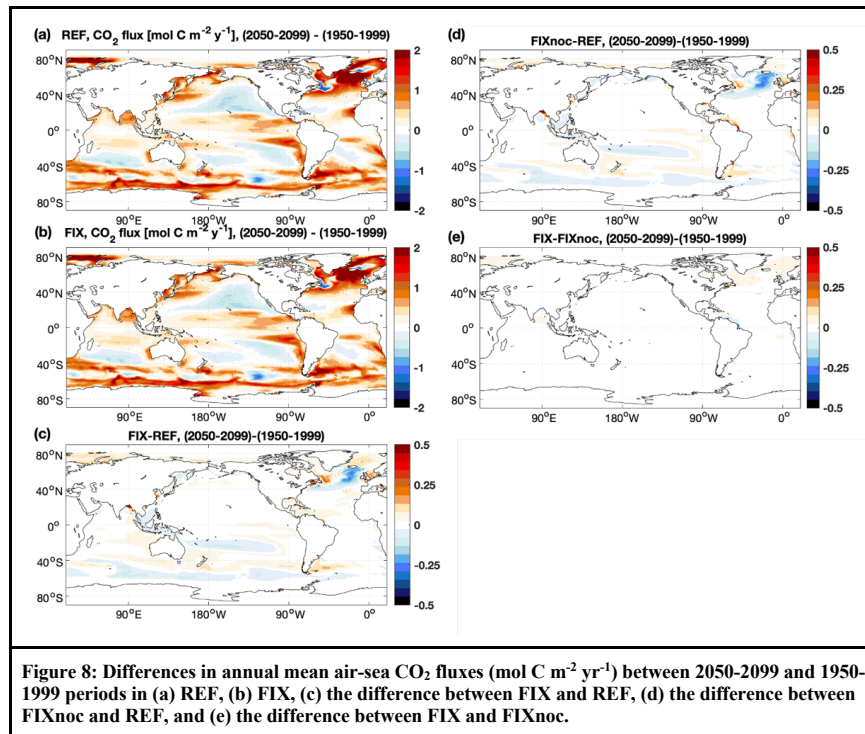


570
 571
 572
 573
 574
 575

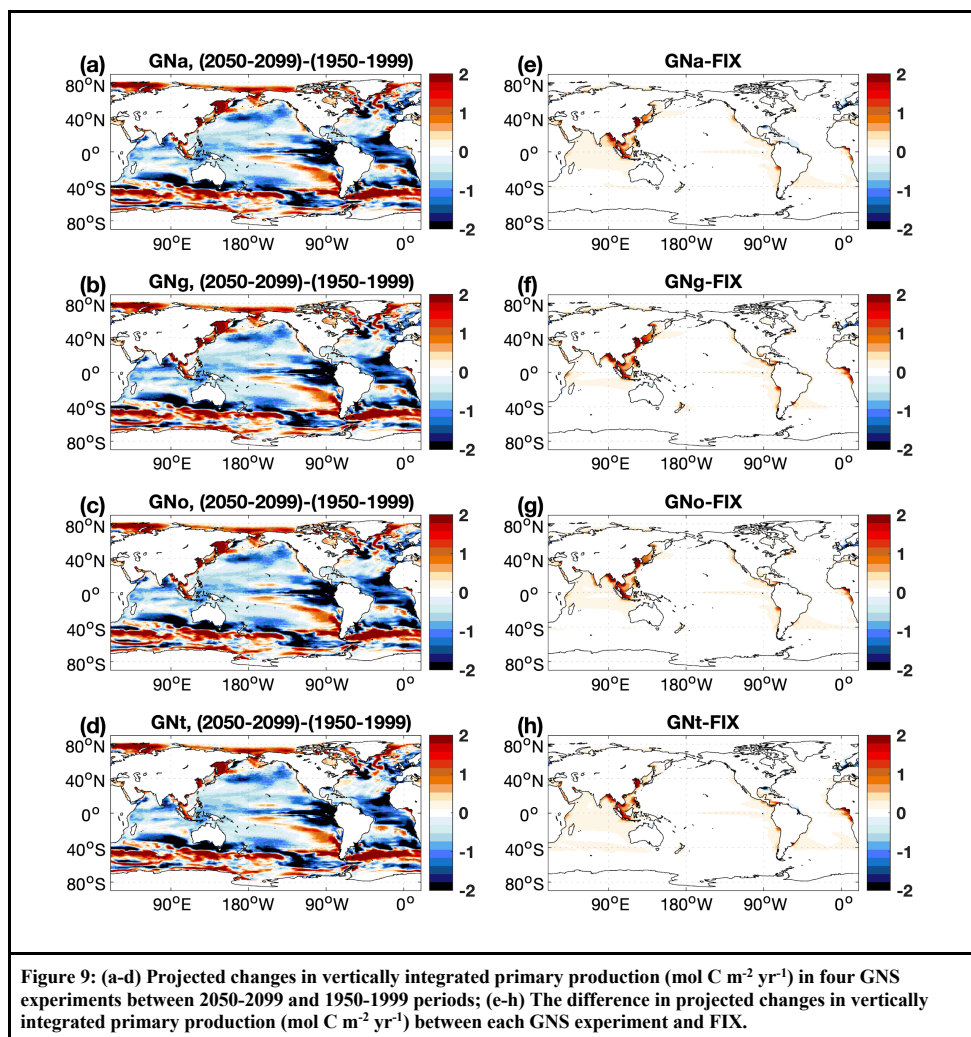




577
 578
 579
 580
 581



582



583
584

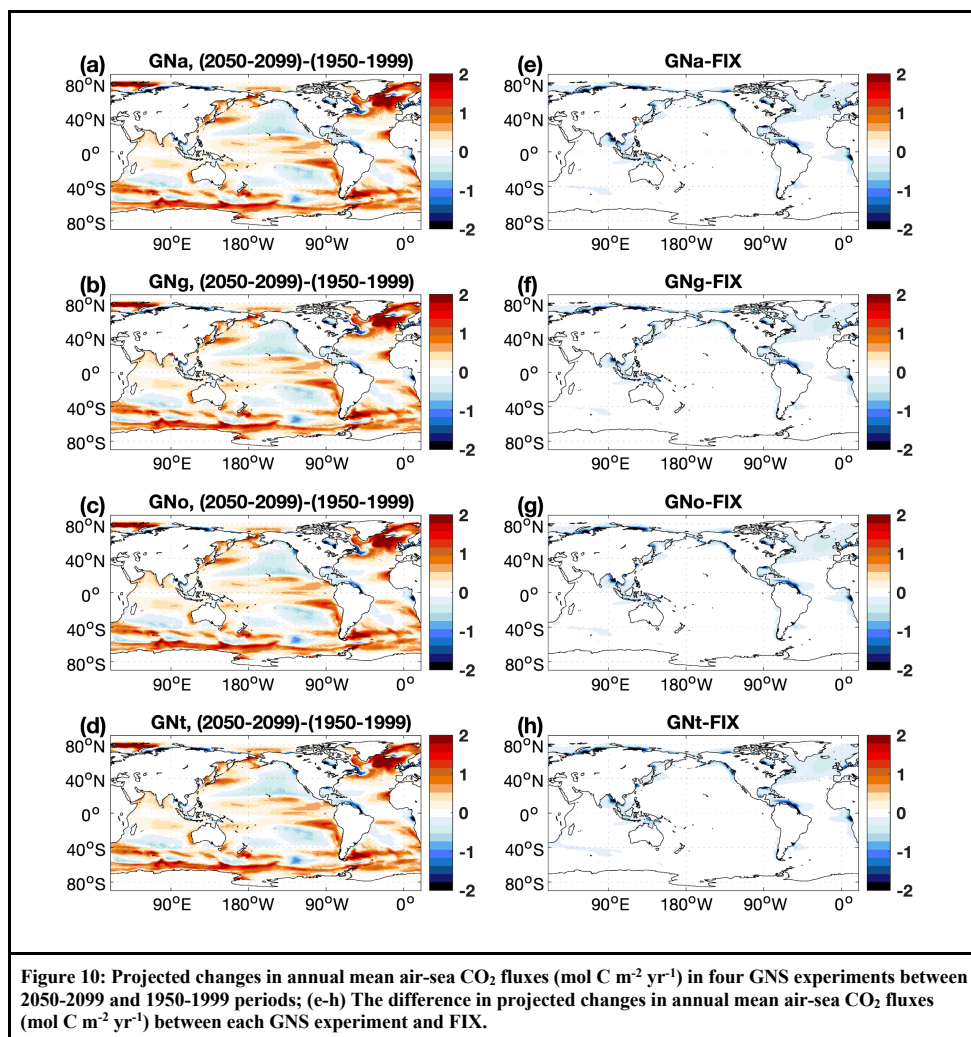


Figure 10: Projected changes in annual mean air-sea CO₂ fluxes (mol C m⁻² yr⁻¹) in four GNS experiments between 2050-2099 and 1950-1999 periods; (e-h) The difference in projected changes in annual mean air-sea CO₂ fluxes (mol C m⁻² yr⁻¹) between each GNS experiment and FIX.

585

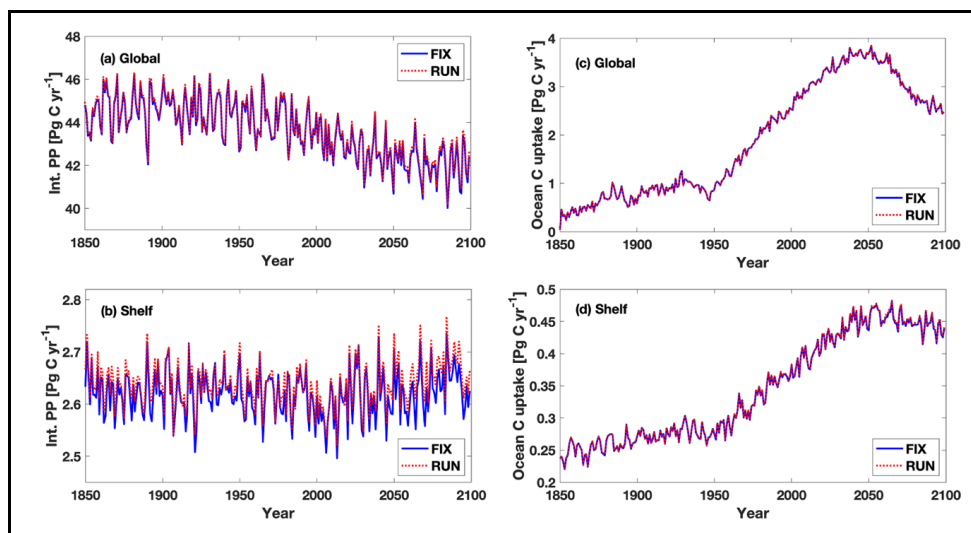


Figure 11: Time-series of integrated annual primary production and ocean carbon uptake during 1850-2099 in FIX and RUN (a, c) globally and (b, d) on continental shelves.

586
 587

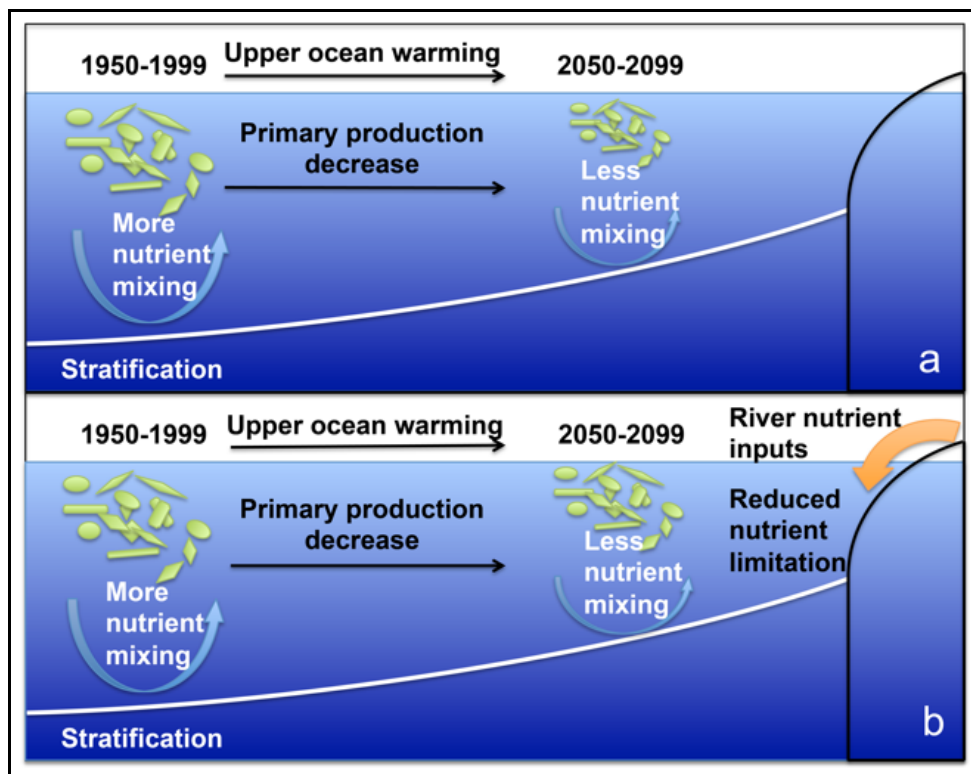




Figure 12: Schematic drawing of impact of riverine nutrient inputs on future projections of marine primary production. Adapted from Aditi Modi (2014) (<http://www.climate.rocksea.org/people/aditi-modi/>). (a) Decline in nutrients supply into subtropical surface waters, due to the upper-ocean warming and increased vertical stratification, is projected by models to reduce primary production over the 21st century. (b) Riverine nutrient inputs into surface coastal waters alleviate the nutrient limitation and lessen the projected future decline in primary production.